DAA / AMES

UCLA-ENG-8532
October 1985

DYNAMIC INSULATION SYSTEMS

By

W.E.W. Chen
W. A. Hepler
S.W.K. Yuan
T.H.K.Frederking

Principal Investigator:
T.H.K. Frederking

PREPARED FOR THE
NATIONAL AERONAUTICS AND SPACE ADMINISTRATION
NASA AMES RESEARCH CENTER
GRANT NAG 2-253

School of Engineering and Applied Science
Chemical Engineering
Department
University of California, Los Angeles
CA 90024

UCLA-ENG-8532
October 1985

DYNAMIC INSULATION SYSTEMS

By

W.E.W. Chen
W. A. Hepler
S.W.K. Yuan
T.H.K.Frederking

WITH "SUPPLEMENT" by J.R. Turner

F I N A L R E P O R T

Principal Investigator:
T.H.K. Frederking

PREPARED FOR THE
NATIONAL AERONAUTICS AND SPACE ADMINISTRATION
NASA AMES RESEARCH CENTER
GRANT NAG 2-253
SUMMER 1985

School of Engineering and Applied Science
Chemical Engineering
Department
University of California, Los Angeles
CA 90024

TABLE OF CONTENTS

PRECEDING PAGE BLANK NOT FILMED

I. INTRODUCTION

A well-established method of insulating systems operating below 300K is the application of "passive" insulation. Systems operating below 50K also usually have a vacuum space with radiation shields. Passive insulation is characterized by the use of low thermal conductivity materials which reduce the heat input into the cold liquid. The method of analysis most frequently employed is the Fourier law of heat conduction. Thus, a low thermal conductivity associated with the heat transfer is required in order to store liquid for long periods of time. As the processes of heat transfer may encompass the three transport modes (conduction, convection, and radiation), the thermal resistance in general is anisotropic. Further, the overall coefficient in Fourier's law constitutes an "effective thermal conductivity" k_e in contrast to the thermal conductivity of a particular material (k). Thus, a complicated pressure, temperature, and geometrical dependence may result.

The insulation technology developed about 30 years ago has relied on vacuum insulated multi-layered radiation shields. In some cases, the effective thermal conductivity exhibits a weak temperature dependance due to the use of particular spacer systems for the shields. The pressure dependance has been evaluated for common systems, and correlations for the optimum spacing have been found. A few years ago, multi-layer insulation (MLI) performance appears to have reached certain limits. Also, the recognition of additional components, such as vent tubes, suspensions, and electrical current leads, as being the major parasitic heat load, has prompted further improvements to give the minimum total heat leak (Q_L). Vapor-cooled radiation shields have led to further lowering of the total heat leak.

In addition, the advent of closed cycle cryocoolers operating down to 20K or lower, has caused further improvements. In this area, the question may be raised regarding which is the better insulation, provided one value of k_e is known* for 25K, for example, and another value is known at 10K. The present studies have the purpose of determining a thermodynamically based evaluation of these types of questions.

------

*) In the subsequent discussion the subscript e in k_e is dropped; k denotes mean values .

II. STATIC VERSUS DYNAMIC INSULATION

The closed cycle cryocooler mentioned previously has been developed in part with the goal of providing a simple thermodynamic tool for the lowering of the temperature in a restricted space. A comparison of this system with the passive insulation suggests that the cryocooler is a "dynamic insulator" when integrated with the usual type of thermal insulation in a cryosystem. In the simplest case, a shield is employed whose temperature is kept low by thermal contact with a cryocooler. There is an additional insulation package between the environmental temperature and the cryo-cooled radiation shield. Additional passive or dynamic insulation may be used between the environment and the cryogenic liquid.

One would like to know about the nature of the two different systems, the passive and dynamic insulation. The former does not require any engine power. The latter does require power in the form of a cryocooler. However, a closer look shows power requirements for the cryoliquid at the production plant. For instance, a minimum amount of work is required per unit mass of liquid. Therefore, it is convenient to determine thermodynamic performance measures based on suitable power ratios. The steps in this direction are outlined subsequently.

III. THERMODYNAMIC PERFORMANCE EVALUATION

This section is divided into two parts. In the first, the general method of thermodynamic performance evaluation is outlined. In the second part, a specific ideal system is selected for illustration.

III.1 General Method

In this work, the approach to a unique thermodynamic performance evaluation is based on the refrigeration power $\dot{W}$, and the work per unit mass $\dot{W}/\dot{m}$. The thermodynamic state dependance of k_e is simplified to $k_e = k_e(T)$ only. For an insulation package of area A, and a thickness d, there is a corresponding thermal conductance $\dot{Q}/\Delta T = \kappa(T)$. However, the use of cryocooler systems will lower the absolute heat input $\dot{Q}_L$ down to a value influenced by $\kappa(T)$. For a specified environmental temperature T_e, one may consider a design specification of the cold temperature T_c. Therefore, the power requirement includes a function of T_e/T_c. If a simple answer is available, one may separate the two contributions to the power, e.g. $\dot{W} = F(\kappa)\cdot f(T_e/T_c)$.

For numerous systems, the exact temperature dependance involved in the function $F[\kappa(T)]$ is not known. Therefore, a constant property approach is convenient at this stage of the studies. The minimum power is now written as

$$\dot{W} = \kappa\cdot f(T_e/T_c) \tag{1}$$

where κ includes the mean thermal conductivity.

For the actual vaporization loss rate, a minimum power $\dot{W}_a$ is needed. Thus, a ratio $\dot{W}/\dot{W}_a$ may serve as the thermodynamic performance ratio

$$\zeta = \dot{W}/\dot{W}_a \qquad (2)$$

When the performance ratio ζ is small, the cryocooler application in principle permits significant improvements. Alternatively, good vapor-cooled shields ought to permit improvements too. When the ratio is large, the insulation is already in a state where improvements are less crucial. The ratio implies that at low temperature, considerable care is necessary. This has been outlined in Appendix A using simplified model assumptions.

Any insulation with vent tubes, supports and other transverse accessories, is worse in the performance than the model insulation analyzed in Appendix A. The actual vessel will require a larger power than the ideal limit of an infinitely large number of cryocoolers. Therefore, the ratio of the vessel's actual ζ-value to the ideal value indicates the overall heat leak conditions of the entire vessel system.

III.2 Ideal Dynamic System

The theoretical frame of reference is illustrated using a sequence of n cryocooler engines or "fridges". The number n is varied from 2 to large n in the limit of an infinitely large number of cryocoolers. The case of n=1 is incorporated by the ideal reference system needed for the liquefaction of a cryogenic liquid.

Consider a two-fridge system, as sketched in figure 3.1 in the temperature-entropy plane (T-S diagram). The following assumptions are introduced: 1. The apparent mean thermal conductivity of the insulation package is constant, and, 2. The area "seen" by the heat flow is constant, and, 3. The insulation thickness is constant. According to Fourier's law, the heat leak is

$$\dot{Q}_{ij} = k(A/d)\Delta T_{ij} \tag{3}$$

or

$$\dot{Q}_{ij} = \kappa\Delta T_{ij} \tag{4}$$

where $\kappa = kA/d$. The heat flows from the "hot" side at temperature T_i to the cold side at temperature T_j. For this system, the fridge has to pump away the incoming heat. For an environmental temperature T_e, and fridge temperature on the cold side of T_j, the minimum power required of each fridge is

$$|\dot{W}_{ej}| = |\dot{Q}_j|(T_e-T_j)/T_k \tag{5}$$

For each stage in the two fridge system, the temperature difference ΔT_{ij} in equation (3) has the set of subscripts ($i=e$, $j=m$) and ($i=m, j=c$). The subscript m denotes the intermediate temperature and c denotes the cryogenic bath temperature. In equation (5), T_k is either T_m or T_c. Inserting the appropriate Q_{ij}-value into the appropriate expressions, one gets a total power of the two-fridge system of

$$\dot{W}_{tot} = \dot{W}_m + \dot{W}_c = \kappa\left((T_c^2/T_m) - 2T_e + T_m\right) + \kappa\left(T_eT_m/T_c + T_c - T_m - T_e\right) \tag{6}$$

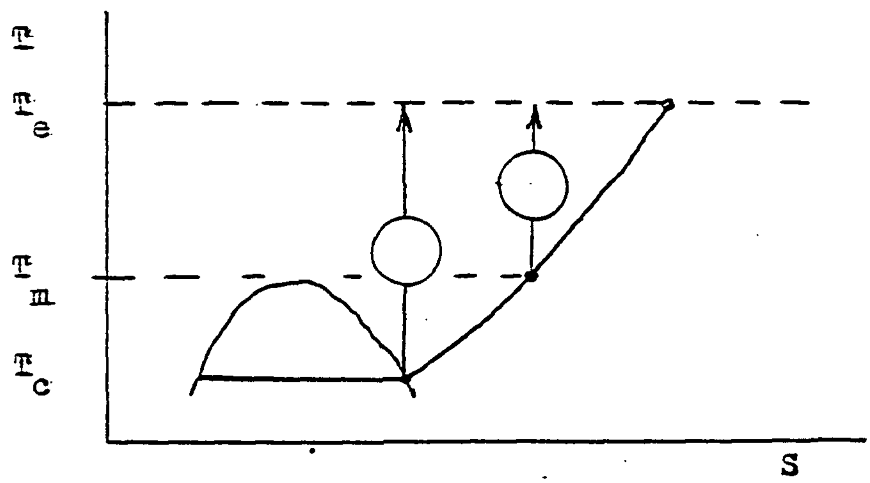

Fig. 3.1. System with 2 cryocoolers in the temperature entropy (T-S) diagram (schematically); Cooler at intermediate temperature takes up heat leak from T_e to T_m ; Cooler at cold bath temperature takes up heat leak from T_m to T_c; (T_e environmental temperature; T_c liquid cryogen temperature).

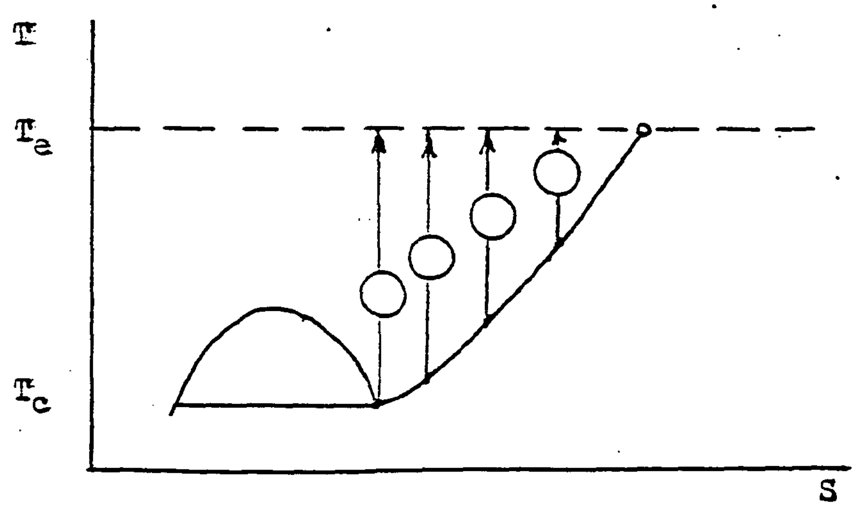

Fig. 3.2. Dynamic insulation system with 4 cryocoolers (schematically) based on ideal Carnot heat pumps ;(T_e , T_c as in Fig.1) .

For the constant properties outlined above, there exists a minimum total power for a particular $T_m = T^*$. Minimization of W_{tot} with respect to T_m, (i.e. $\partial W_{tot}/\partial T_m = 0$) leads to an optimum temperature

$$T^* = \sqrt{T_e T_c} \tag{7}$$

or the temperature ratio is

$$T^*/T_e = T_c/T^* = \sqrt{T_e/T_c} \tag{8}$$

The total power associated with this minimum is determined readily by inserting T^* into equation (6) to get

$$W^* = \kappa\left(T_e(T_eT_c)^{\frac{1}{2}}/T_c - T_e + T_c - (T_eT_c)^{\frac{1}{2}}\right) \tag{9}$$

It is noted that for $T_e = 300$ K and for $T_c = 3$ K, the optimum T^*-value which minimizes the total two-fridge power is 30 K.

The calculations are carried out readily for the three-fridge system, or the four-fridge system. For details of the numerical illustrations, we refer to the Supplement. Taking a slightly different approach, we arrive at the optimum T-ratio by induction. For the n-fridge system, the optimum temperature ratio which minimizes the total power is

$$(T_{m+1}/T_m)_n = (T_e/T_c)^{1/n} \tag{10}$$

There are (n-1) intermediate temperatures, optimized to reduce the fridge power to its minimum value. The subscripts m and m+1 denote successive optimum temperatures, as T is lowered.

Finally, in these ideal system calculations we turn to hypothetical case of an infinite number of cooler systems.

This special limit may be obtained in a straightforward manner using the method of differential Carnot processes. The heat leaking from stage k-1 to stage k is

$$d\dot{Q} = \kappa dT \tag{11}$$

The differential work of a differential Carnot cycle for stage k is* $dW \sim dQ$, or

$$d\dot{W} \approx d\dot{Q}(T_e - T)/T \tag{12}$$

After substitution of equation (11) into (12), the total power of the system of coolers is obtained by integration

$$\dot{W} = \int d\dot{W} = \kappa\left(T_c \ln(T_e/T_c) - (T_e - T_c)\right) \tag{13}$$

Thus, a rather simple result is obtained for this hypothetical limit of a dynamic insulation system (ideal case of constant properties). It may be noted that the thickness will vary for the total system. However, only a few layers of super-insulation are needed when there is a very small temperature difference between adjacent shields. This does not cause great difficulties. In the practical implementation, only a limited number of cryocoolers or stages will lead to an economic optimum which minimizes the total cost of operation and investment. Further details will be discussed after the next section describing the experiments conducted.

*) Power is characterized by a dot denoting the derivative with respect to time.

IV. EXPERIMENTS

Experiments have been conducted with foam insulated containers. A cylindrical vessel and a large rectangular box were used. The interior liner of both containers is a stainless steel sheet metal system welded on all seams.

The cylinder run was designated as experiment #1. Foam #1 is polyurethane and had a height of 40.4 cm and a radial thickness of 7 cm. During the experimental runs, a very thick polyurethane cover was used. The cover was cooled to liquid nitrogen temperature prior to the run so that no heat transfer from the top could be assumed in the subsequent data analysis. The temperature of the inside stainless steel wall below the liquid level was assumed constant at the boiling point of liquid nitrogen. Copper—Constantan thermocouples were attached to the stainless steel liner at 2 cm and 11 cm below the top rim. The reference temperature was that of liquid nitrogen boiling at 77 K. The thermocouple signal was monitored with a Fluke 2240A Datalogger. The liquid nitrogen level was observed and is presented versus temperature in figure 4.1

The runs shown in figure 4.1 were conducted on three different days starting from an initially warm container. After the initial period of about one hour, the data indicate quasi-steady-state conditions. The initial removal of foam enthalpy and possibly the latent heat of condensation or

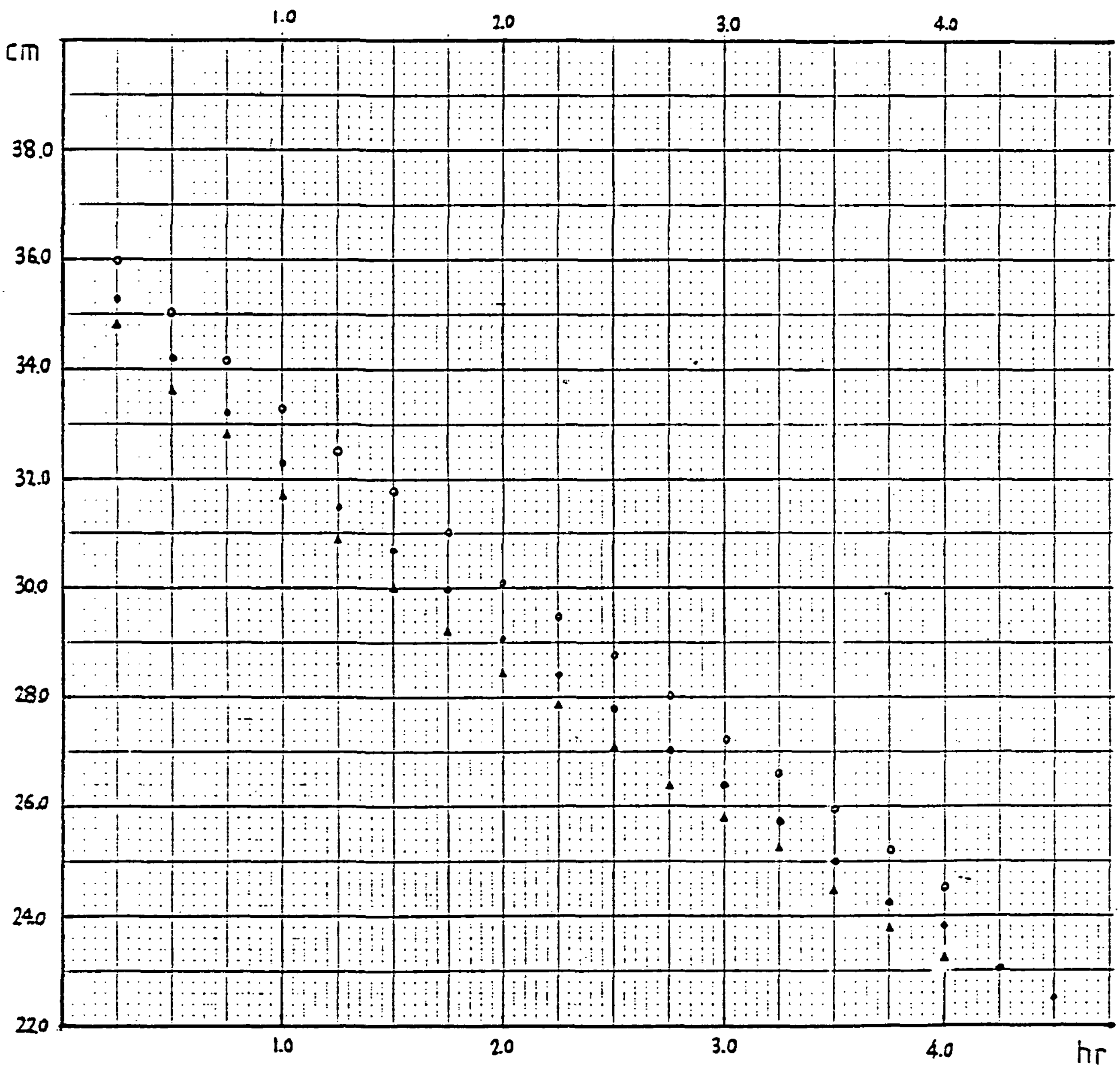

Fig.4.1. Liquid level versus time ;(Foam # 1)

fusion of condensible gases in the foam material is seen to cause an initially steep change of the liquid level with time.

Figure 4.2 displays the liquid level versus time for the rectangular box (experiment #2). The box inside dimensions were 55.7 by 56 by 35.5 cm. The thickness of the foam was 10 cm. Runs on two different days are shown in figure 4.2. The attachment of the foam to the stainless steel liner on the first run was defective allowing relative motion and an enhanced heat leak due to convection. For the second run, the foam sections were fastened reliably. This caused the data to show a lower heat leak which varied little with time.

Data reduction was done using Fourier's law for steady heat flow. The actual heat leak $\dot{Q}_a$ is expressed in terms of a mean (apparent) thermal conductivity (k).

$$\dot{Q}_a = (A/d)k\Delta T = \kappa\Delta T \tag{14}$$

where d is the thickness and A is the area. The temperature difference is $\Delta T = T_e - T_c$ where $T_c = 77$ K and $T_e \simeq 300$ K. The mean value of the thermal conductivity is obtained from equation (14).

$$k = (d/A)\cdot(\dot{Q}_a/\Delta T) \tag{15}$$

The actual heat leak was determined from the rate of change of the liquid level with time, relying on the late-stage time period with quasi-steady-state change of liquid

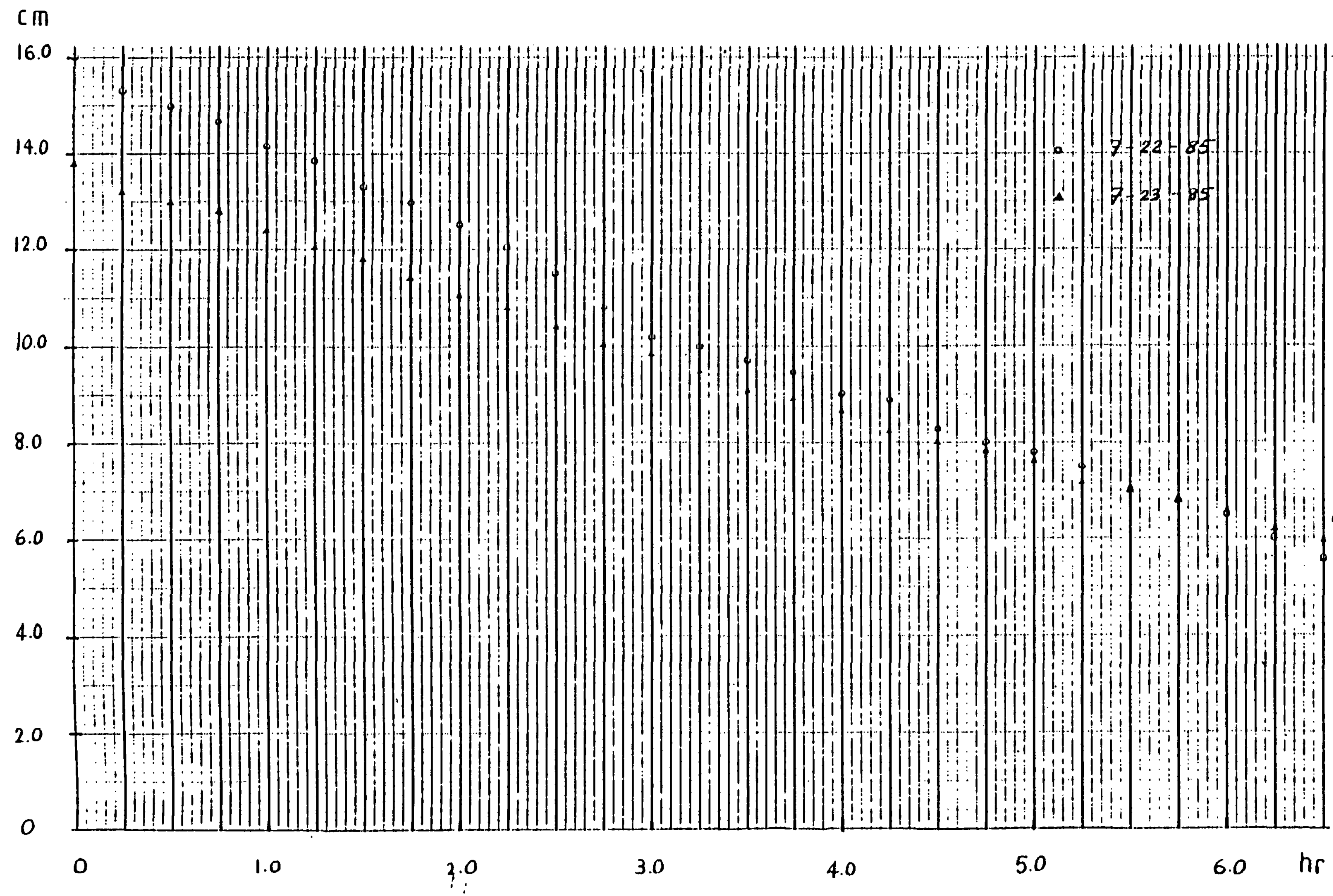

Fig. 4.2. Liquid nitrogen level versus time ; (Form # 2)

ORIGINAL PAGE IS
OF POOR QUALITY

level with (dz/dt). From the cross-sectional area A_c, the volumetric change $\dot{V} = A_c(dz/dt)$ is obtained and from the density (ρ) and the latent heat of vaporization (λ), $\dot{Q}_a$ is determined from the following equation.

$$\dot{Q}_a = \lambda\rho\dot{V} \tag{16}$$

The foam thermal conductivity results are included in figure 4.3 which also contains the literature data of Mori and Shingen[1]. The PVC sample of these authors shows a weak temperature dependance of the thermal conductivity. The polyurethane foam, designated as PUF, indicates an increase in k as the temperature is lowered from about 265 K to 220 K. The reason for this phenomenon was not given by Mori and Shingen. It is suspected that the possibility of vapor condensation may exist in this temperature range

The mean thermal conductivity value obtained for foam #1 (dashed line) appears to be in good agreement with the data of these authors. The PVC data indicates the possibility that an initially higher mean temperature during the present runs may cause an enhanced heat leak. The foam #2 shows a larger mean thermal conductivity possibly caused by some open pores and cracks with localized convection.

The insulation performance has been deduced using the parameter n as the performance measure (equation (2)). The ideal reference power is from equation (13). The minimum liquefaction work required is[2] $\dot{W}_{liq}/\dot{m} = 0.213$ kWhr/kg = 766.8 J/g

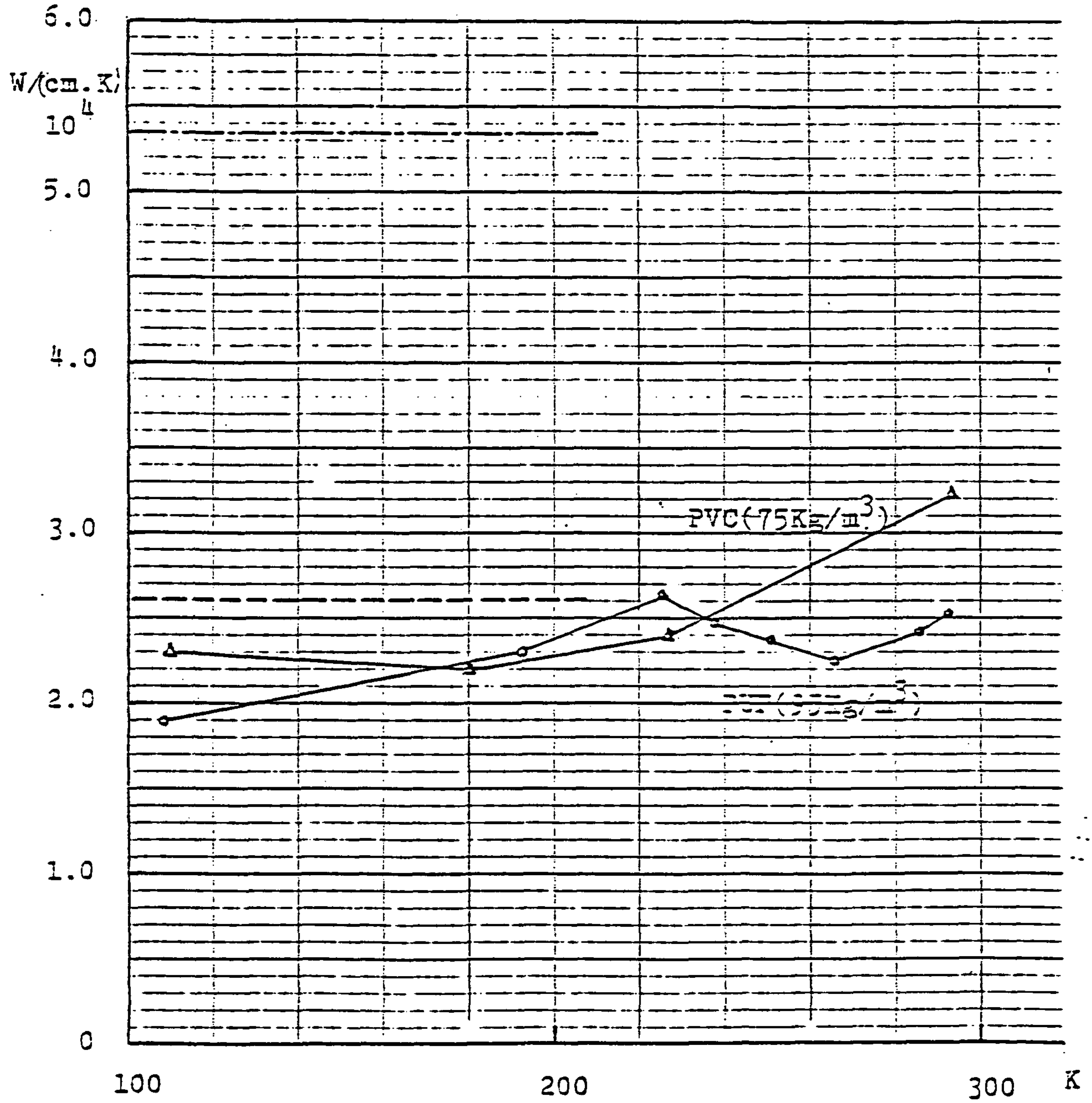

Fig.4.3. Thermal conductivity versus temperature

——— Mean value of foam # 1

———·— Mean value of foam # 2

The foam thermodynamic performance values are listed in Table 4.1.

Liquid nitrogen data have been taken observing the liquid level change in vacuum insulated vessels (160 liter capacity, MVE Type 405, TW 207, specified as 9/68 and 4/73). Another vessel with the same volume had the specification MVE 684. The liquid level change with the vessel pressurized to 28 psig versus time is shown in figure 4.4. Figure 4.5 contains data taken with depressurized liquid nitrogen at the normal boiling point. Another similar run is shown in Figure 4.6. Figure 4.7 gives the rise of the vessel pressure with time, when the vent valve is closed after the tank had been depressurized to 1 atm.

The rate of liquid loss with time indicates a heat leak of the order of magnitude 1 liter per day. For the liquid nitrogen density of 0.8 g cm^{-3} and a latent heat of 200 J/g, the heat leak is of the order of magnitude 2 W. For these vessels, only the order of magnitude is given because of the lack of exact container details.

For the design aspects of insulation systems for containers, the approach along the line of Appendix A is taken. The appendix discusses the container with a hypothetical insulation package without supports, neck tubes, or other components. This package has less heat leak, i.e. lower required refrigeration power, than the actual container. The insulation is characterized by its κ-value. For the

Table 4.1.

FOAM RESULTS

#	Actual heat leak $\dot{Q}_a = \lambda \dot{m}$ W	Refrigeration power $\dot{W}_\infty$, W	Ratio ζ_{in}
1	14.3	12	0.22
2	169	140	0.21

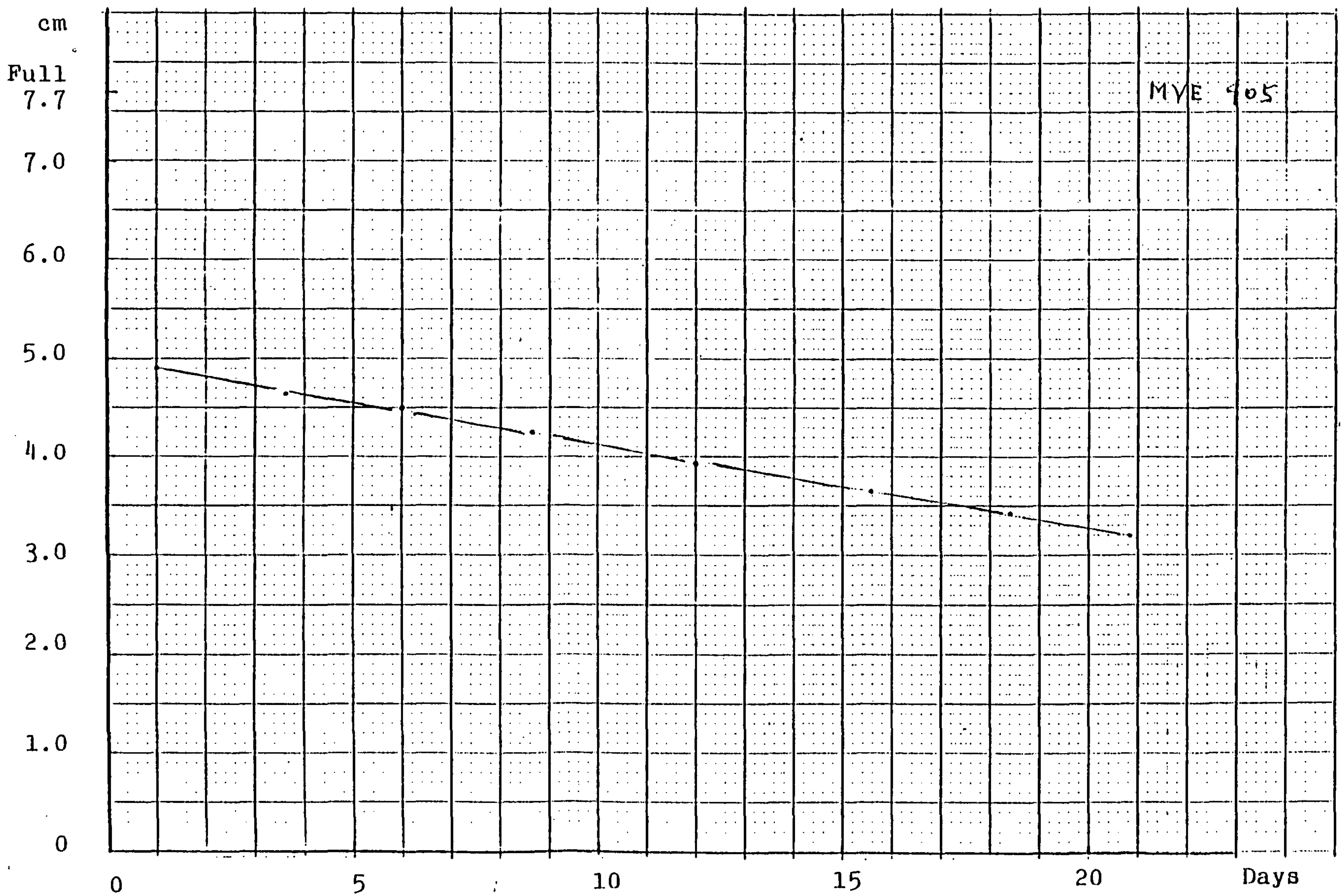

Fig.4.4. Level indicator of a 160 liters Vacuum insulated tank versus time

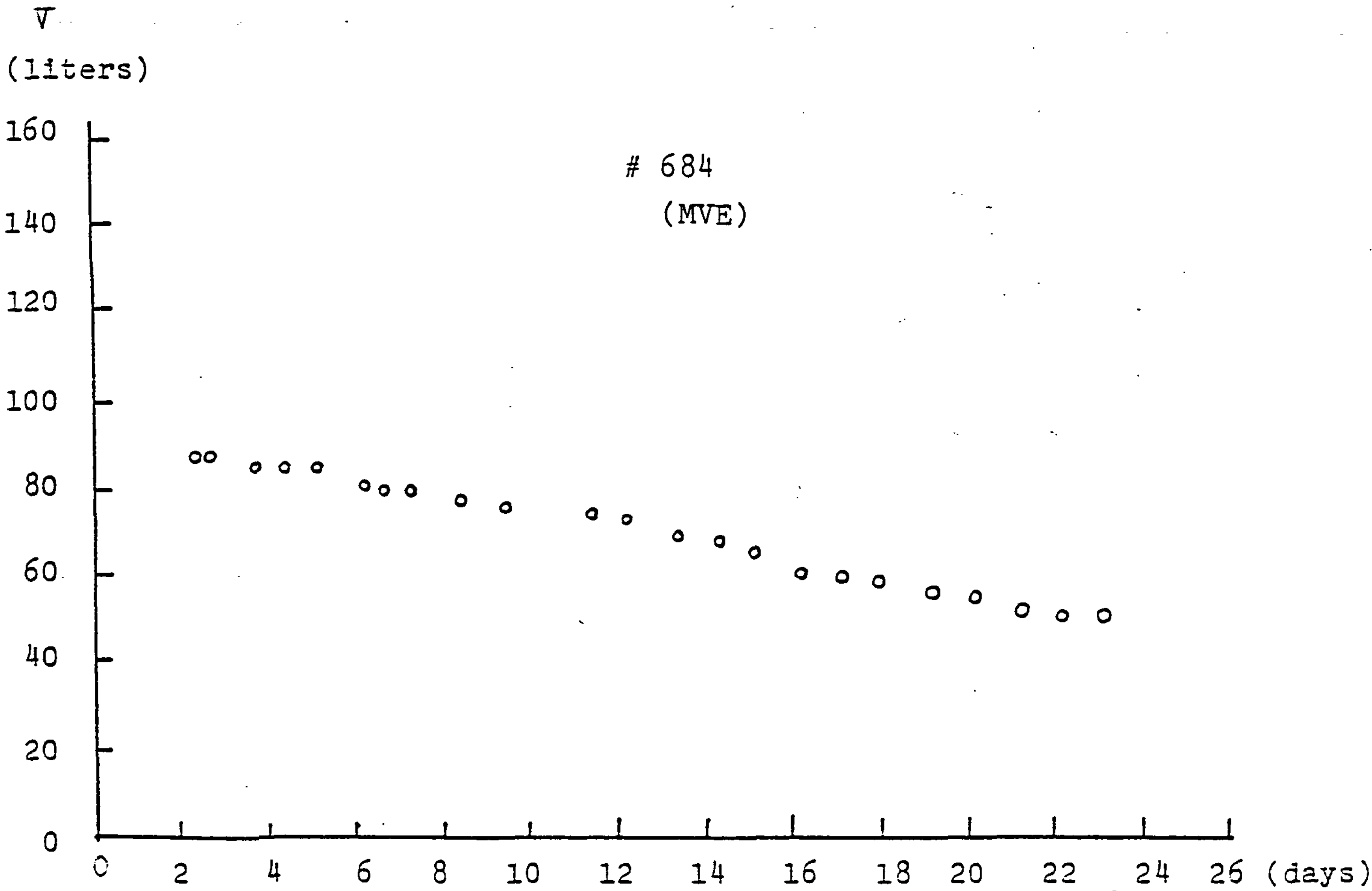

Fig.4.5. Liquid nitrogen volume versus time

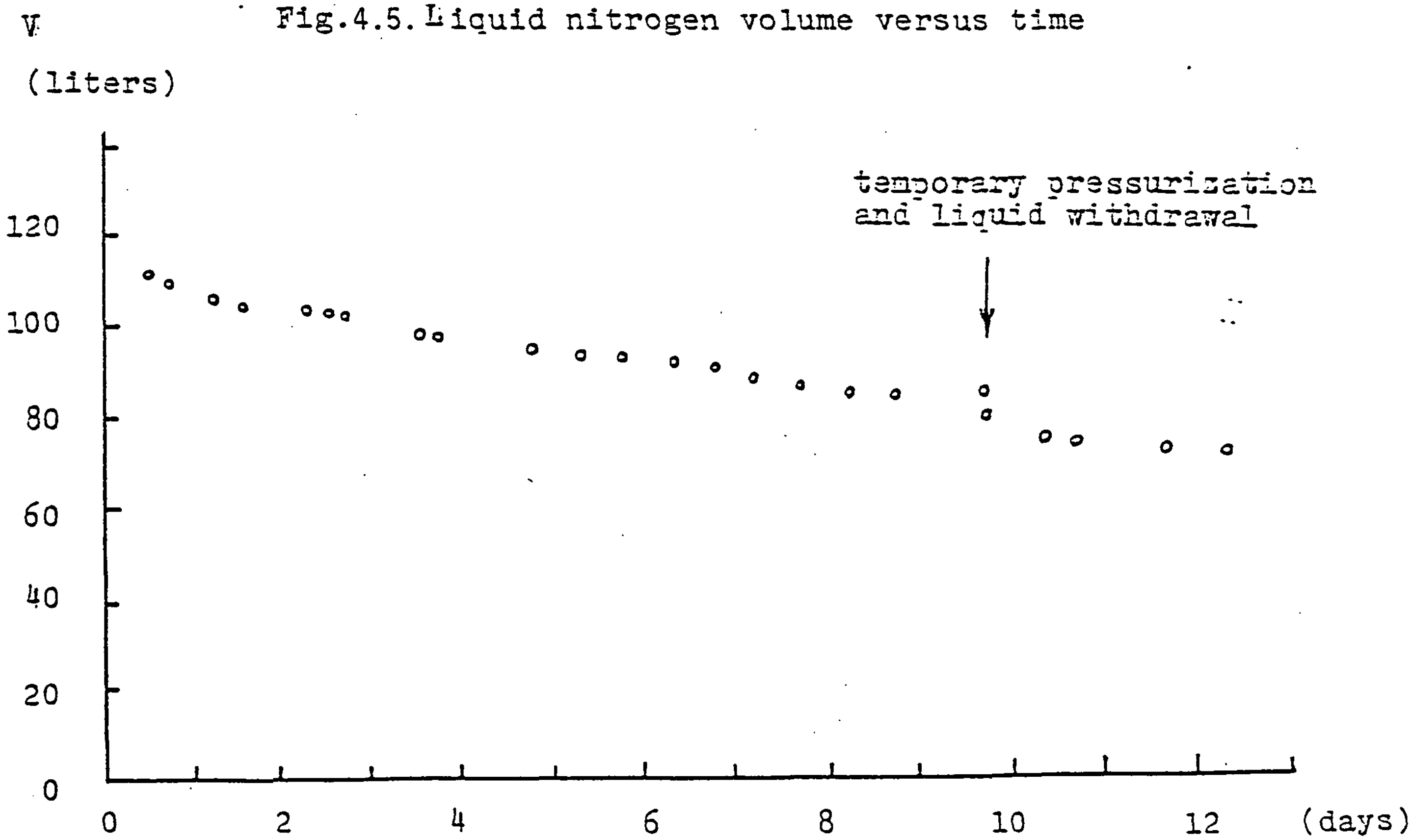

Fig.4.6. Liquid nitrogen volume versus time

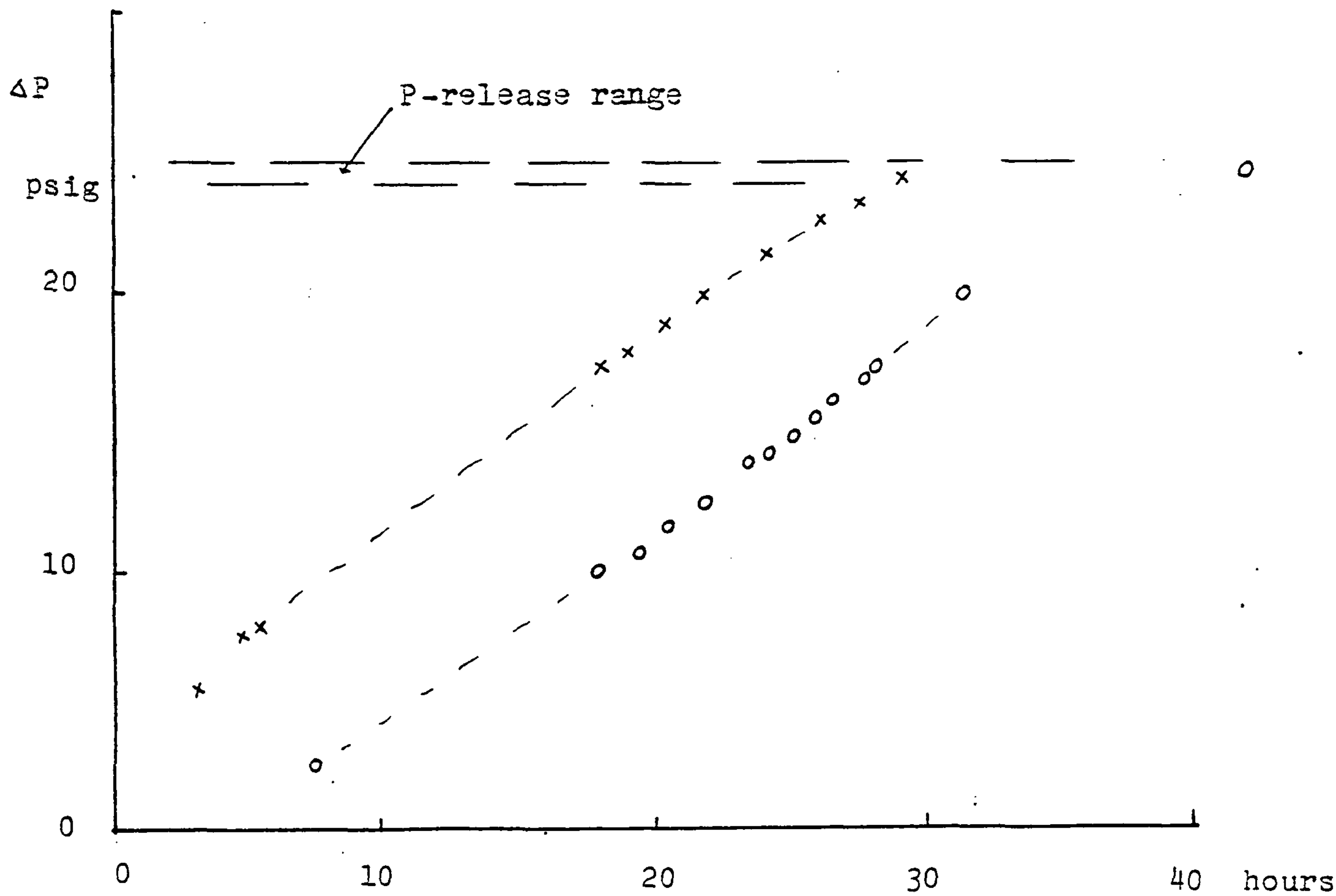

Fig.4.7 . The pressure as a function of time during pressurization caused by the heat leak into the tank.

x Run # 1 ;

o Run # 2 .

160 liter liquid nitrogen container, the order of magnitude of the container area is about $17 \cdot 10^3$ cm^2, the thickness is estimated to be of the order 2 cm. The superinsulation k-value is assumed to be of the order 10^{-6} W/(cmK). The resulting κ-value is of the order of 8 mW/K. The minimum reference power for an infinitely large number of cryocoolers is $\dot{W}_\infty = \dot{m}_L W_\infty^0$ of the order of 1 W. The related liquefaction power required is $(\dot{Q}_a/\lambda)(\dot{W}_{liq}/\dot{m}) \sim 8$ W. The resulting η-value is of the order 20%.

A similar assessment is given for a 100 liter liquid He^4 storage container. The order of magnitude of the area is $11 \cdot 10^3$ cm^2. For a thickness of the order 2.5 cm, and for a mean k(T)-value of $k \sim 10^{-6}$ W/(cm K), ζ of the order of 5 mW/K is obtained. The typical boiloff of the conventional container is 1 % of the volume per day, i.e. 1 liter / day . This corre - sponds to a heat leak of the order of 30 mW , and to a mass flow rate $\rho V = \dot{m} = \dot{Q}_a/\lambda$ of the order 1 mg/s . The ideal power per mass flow rate $(= W_{liq}/m)$ has been given by Barron as 1.894 kWhr/kg = 6818 J/g. The resulting reliquefaction power is of the order of 10 W . From the present dynamic system model we obtain the optimum W_{oo} associated with the (hypo - thetical) use of an infinitely large number of cryocoolers. This power has the order of 5 W 10 W. The related effective- ness becomes 0.5. Appendix A lists a thermodynamic ζ-value of 0.01. Any higher heat leak into the 100 liter vessel will lower the effectiveness.

V. DISCUSSION AND CONCLUSIONS

The topics considered are 1. The characterization of the supportless insulation ; 2. The discussion of container data; and 3. The conclusions.

V.1. Characterization of supportless insulation . In this area we may distinguish the non-cryogenic insulation of low cost and the "high-tech" insulations of an advanced nature aiming at the lowest possible parasitic heat leak into a tank. The conventional insulation is to be cheap. Therefore, sophisticated "dynamic" approaches are ruled out.

In the high-tech area, the two major categories are vapor-cooled shield systems without cryocoolers, and dynamic systems with cryocooler use. Both options may reach quite a low parasitic heat leak. On economic grounds one may rule out any sophisticated system with a large number of cryocoolers .(Also noise considerations may play a role). Therefore, the vapor-cooled system, known from aerospace applications, may be a serious competitor in liquid He^4 storage vessel approaches. As discussed in App. A, the supportless system has thermodynamically determined ζ -values which depend on temperature, i.e. the boiling point of concern. The real vessel's parasitic heat input is characterized in the present approach using the insulation effectiveness ε . This power ratio ought to permit a useful comparison between the two high-tech categories of insulation including supports and ducts.

V.2. Discussion of Container Data

The results obtained with liquid nitrogen vessels indicate for the best cases that ε may be rather close to unity. If energy prices are not rising significantly, this situation appears to offer much less incentives for improvements of $l.N_2$ tanks than for liquid Helium vessels.

In the liquid Helium sector, there are significant differences from one design to another. Further, the performance ratios ε have been found to be quite for the storage vessels in the usual distribution systemd. Thus, the question of an intercomparison on the basis of a thermodynamic parameter appears to be quite attractive. Though the numbers obtained are only approximate , the low effectiveness values seem to invite further evaluations for the two categories mentioned in Sec. V.1.

V.3. Conclusions

The initial results obtained in the present studies indicate that a thermodynamic approach is quite useful, in particular for low boiling liquids , such as liquid hydrogen and the helium liquids. The method proposed appears to offer the opportunity to calculate performance when one parameter is changed. The thermodynamic nature of our approach is sufficiently general to replace the usual empirical discussion of parasitic heat leak measures , such as absolute boiloff rates.

REFERENCES

1. T. Mori and Y. Shingen, Conf. Proc. SCEC'85, Shanghai, June 1985, Pt. B, pp. 155-158.

2. R. Barron, Cryogenic Systems, McGraw-Hill, New York, 1966.
   R.F. Barron, Adv. Cryog. Eng. Vol. 17, 1972, p.20 ;
   R.F. Barron, Cryogenic Systems, 2nd Ed. 1985, p. 63.

ACKNOWLEDGEMENT

We are acknowledging the help of Vladimir Valentekovich and John Van Zanten during the initial foam experiment preparation.

Appendix A. Simplified Cryovessel System: Insulation Without Neck Tube System

Consider an ideal system characterized by a lack of neck tube, support members, vent ducting (other than low conductivity vapor cooling connectors between shields). Thus, complete insulation coverage of the vessel is treated as a suitable reference case with quasi-uniform insulation (not necessarily isotropic). The heat leak to the insulation is $\dot{Q}_{aL}$. It requires a minimum power $\dot{W}_L$ in order to reliquefy the boiloff. The mass flow rate of vapor is

$$\dot{m}_L = \dot{Q}_{aL} / \lambda \qquad (A.1)$$

(λ latent heat of vaporization). Once a suitable insulation ("superinsulation") is available, the reference system is designed readily :

$$\dot{Q}_{a_L} = \varkappa (T_e - T_c) \qquad (A.2)$$

For the volume specified, the area A is available, once the vessel shape has been selected. For the adopted thickness and insulation type, the $\varkappa$- value is fixed ($\varkappa = k\ A/d$). The minimum liquefaction power is readily available, and it is noted that text books give values of the liquefaction work (W_{liq}/m), per unit mass, for various NBP

$$(W_{liq}/m) = T_e(S_c - S_e) - (H_e - H_c) \qquad (A.3)$$

S is the entropy per unit mass; H enthalpy. The subscript e denotes "environment", e.g. 1 atm , 300 K . The subscript c denotes NBP conditions. For cryogenic liquids of low boiling point, the assumption of a constant specific heat is a reasonable approximation. Therefore, (W_{liq}/m) may be expressed as

$$(W_{liq}/m) = T_e\, c_p \ln(T_e/T_c) - c_p(T_e - T_c) + (\lambda/T_c)\, T_e - \lambda \qquad (A.4)$$

For liquid He^4 , in particular, the latent heat is small compared to $c_p(T_e - T_c)$. Therefore, a good first order approximation is

$$(W_{liq}/m) = T_e\, c_p \ln(T_e/T_c) - c_p(T_e - T_c) \; ; \qquad (A.5)$$

$$T_{ref} = \lambda/c_p \ll (T_e - T_c)$$

After insertion of the preceding information into the definition for the performance measure of an insulation package (ζ) , we evaluate numerical results. We have

$$\zeta = \dot{W}_\infty / [\dot{m}_L \, (W_{liq}/m)] \qquad (A.6)$$

Insertion of Eq. (A.1) into (A.6) leads to

$$\zeta = \lambda \cdot \dot{W}_\infty / \left[\dot{Q}_{aL} (W_{liq}/m) \right] \qquad (A.7)$$

A particularly simple result is obtained for He^4 using $\dot{W}_o = \dot{W}^o_\infty \, \dot{m}_L$, Eq (1) and (A.2), (A.5) in (A.7) : $\zeta \rightarrow \tilde{\zeta}$

$$\tilde{\zeta} = \frac{\lambda}{c_p\,(T_e - T_c)} = T_{ref}/(T_e - T_c) \qquad (A.8)$$

If the latent heat is not small, the assumption of constant specific heat* may be retained using Eq. (A.4) for the determination of ;

$$\zeta = \frac{\lambda \quad \left\{(T_e \cdot \ln(T_e/T_c) - (T_e-T_c)\right\}}{(T_e - T_c)\left[T_e\left\{c_p \ln(T_e/T_c) + (\lambda/T_c)\right\} - \left\{c_p(T_e-T_c) + \lambda\right\}\right]}$$

(A.9)

It is noted that the performance measure of the insulation is quite a pronounced function of the NBP, i.e. the T_c-value, when cryo-liquids are stored at 1 atm. The smaller the NBP , the larger (T_e-T_c) will be, approaching T_e at low temperatures . At the same time, T_{ref} becomes small, as the latent heat is no longer described by Trouton's rule . The quantum effects "blow up " the liquid volume, and less energy is needed to bring the latoms (molecules) from the saturated liquid state to the saturated vapor state. As a result , the performance measure decreases significantly as T_c is lowered.

Because of the lowering of ζ with a decrease of the NBP, it appears to be useful to measure ζ with respect to the present reference value of the insulation package proper; e . g .

$$\zeta_{in} \equiv \zeta / \varepsilon \qquad (A.10)$$

----

*) For a rigorous evaluation , the state functions S,H (Eq. A.3) ought to be considered.

This definition of the effectiveness $\varepsilon = \zeta / \zeta_{in}$ measures the actual cryo -system performance,(including support , neck tube and other contributors to $\dot{Q}_a$), with respect to the "tubeless" case. It requires a detailed knowledge of the insulation system in order to arrive at improvements of ε.

Table A.1 lists selected values of ζ for T_a = 300 K. ($\tilde{\zeta}$ denotes the simplified result A.8).

Table A.1
"Tubeless" Insulation Package Performance , ζ, $\tilde{\zeta}$
Eqs. A.8 , A.9 for Selected Cryo-Liquids

	NBP , K	** Lat.Heat λ ,J/g	** cp J/ (g K)	$\tilde{\zeta}$	ζ
l.N_2	77	199.1	1.03	0.37	.21
l.H_2 x)	20	446.5	10.3	0.155	.072
l.He^4	4.2	20.91	5.23	0.0135	.0105

----
x) p-H_2

**) Basis: G. Klipping, Tabulation ;
T_a = 300 K.

Supplement: System With j Cryocoolers

Jay R. Turner

A discussion of the j-stage system is given. The various terms are illustrated using an environmental temperature of T_e = 300 K and a cold bath temperature of 3 K.

Consider a system containing j cryocooler stages. The minimum power required is written for optimum T-values of the various shields, as

$$(W^*/\varkappa) = \sum_{i=1}^{j} T_e T_{j+1}/T_i - (1+j)T_e - T_c \qquad (S.1)$$

The optimized intermediate temperatures are expressed as

$$T^*_{mi} = (T_e^{\,i-1}\, T_c^{\,j-i+1})^{1/j} \qquad (S.2)$$

First the variation of the normalized power with the intermediate shield temperature T_m is discussed for the two-cryocooler system. The dimensionless power is shown in Figure S.1. It is seen that the power $W^o = W/\varkappa$ is varying relatively weakly near the optimum temperature of 30 K.

As soon as the number of cryocoolers is increased, one may vary more than one intermediate temperature. This variation may cause more complicated effects. However, in line with similar optimization procedures, the system becomes less sensitive to small departures of shield temperatures from their optimum values. Examples of the numerical calculations are given for various j-values, as follows; (T_e = 300 K, T_c = 3 K).

<u>j = 1</u> : Dimensionless work $W^o{}_1 = T_e^2/T_c - 2T_e + T_c$

$W^o{}_1$ = 29 403 Dimensionless Units

<u>j=2</u> : Optimum intermediate $T^*_m = (T_e^1\, T_c^1)^{1/2}$

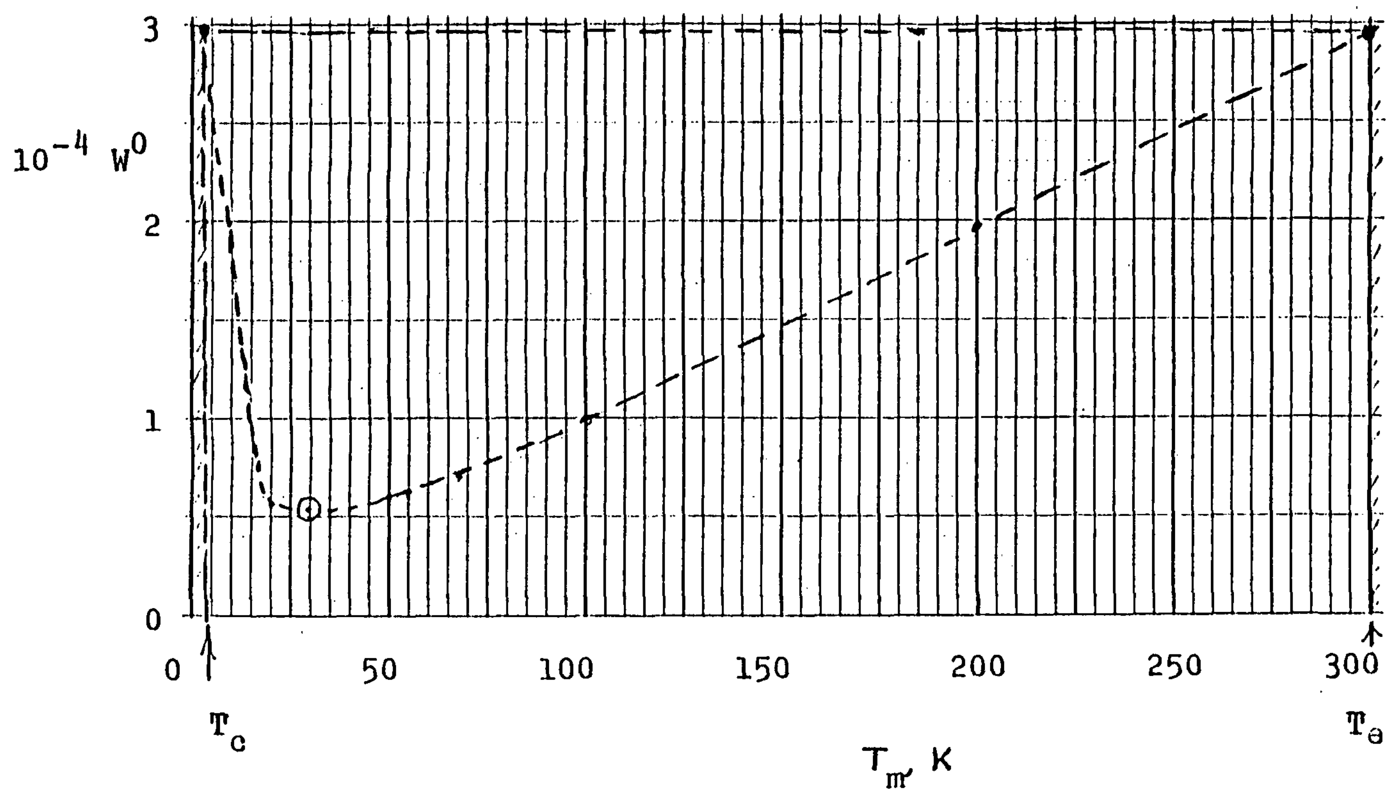

Fig. S.1. Dimensionless power required for a two-cooler system when the intermediate temperature T_m is varied.

j = 2 (continued): $T_2^* = 30$ K ;

Dimensionless power $W^o = T_e T_2^*/T_c - T_e T_e/T_2^* - 3T_e + T_c$

$= 5103$

j = 3

In the subsequent listings, the superscript * denoting the optimum value is dropped. Instead, various optimum shield temperatures are labelled sequentially, e.g. T_2 , T_3 .

Optimum intermediate T-value:

$$T_i = (T_e^{\,i-1}\, T_c^{\,j-i+1})^{1/j}$$

$$T_2 = (T_e^{\,2-1}\, T_c^{\,3-2+1})^{1/3} = (T_e\, T_c^2)^{1/3} = 14 \text{ K} .$$

$$T_3 = (T_e^{\,3-1}\, T_c^{\,3-3+1})^{1/3} = (T_e^2\, T_c)^{1/3} = 65 \text{ K} .$$

Work value:

$$W^o = T_e T_2/T_c + T_e T_3/T_2 + T_e T_e/T_3 - 4\,T_e + T_c$$

$$= 2980 .$$

j = 5

The four intermediate temperatures are:

$$T_2 = (T_e T_c^4)^{1/5} = 7.5 \text{ K}$$

$$T_3 = (T_e^2\, T_c^3)^{1/5} = 18.9 \text{ K}$$

$$T_4 = (T_e^3\, T_c^2)^{1/5} = 47.5 \text{ K}$$

$$T_5 = (T_e^4\, T_c)^{1/5} = 119.4 \text{ K} .$$

The optimum power value is $W^o = 1971$

j = 10

The following list of optimum intermediate temperature results :

$T_2 = (T_e\, T_c^9)^{1/10} = 4.8$ K

$T_3 = (T_e^2 T_c^8)^{1/10} = 7.5$ K

$T_4 = (T_e^3\, T_c^7)^{1/10} = 11.9$ K

$T_5 = (T_e^4\, T_c^6)^{1/10} = 18.9$ K

$T_6 = (T_e^5\, T_c^5)^{1/10} = 30.0$ K

$T_7 = (T_e^6\, T_c^4)^{1/10} = 47.5$ K

$T_8 = (T_e^7\, T_c^3)^{1/10} = 75.3$ K

$T_9 = (T_e^8\, T_c^2)^{1/10} = 119.4$ K

$T_{10} = (T_e^9\, T_c\,)^{1/10} = 189.3$ K .

The dimensionless power is 1458

The sequence of optimum intermediate temperatures is shown in Fig. S.2 versus the j-values for the T_c and T_e adopted in the present calculations. The temperatures are logarithmically distributed about T = 30 K.

The optimum power figures, in dimensionless form, are displaced in Fig. S.3 versus j . The asymptotic value for an infinitely large j is

$$W^o_\infty = T_e \ln(T_e/T_c) - (T_e - T_c) = 1085$$

It is seen in Fig. S.3 that there is an initial steep decrease of the power values when j is increased . Beyond j = 4, the variation of W^o with j is less pronounced. Beyond j = 10, very little change is observed.

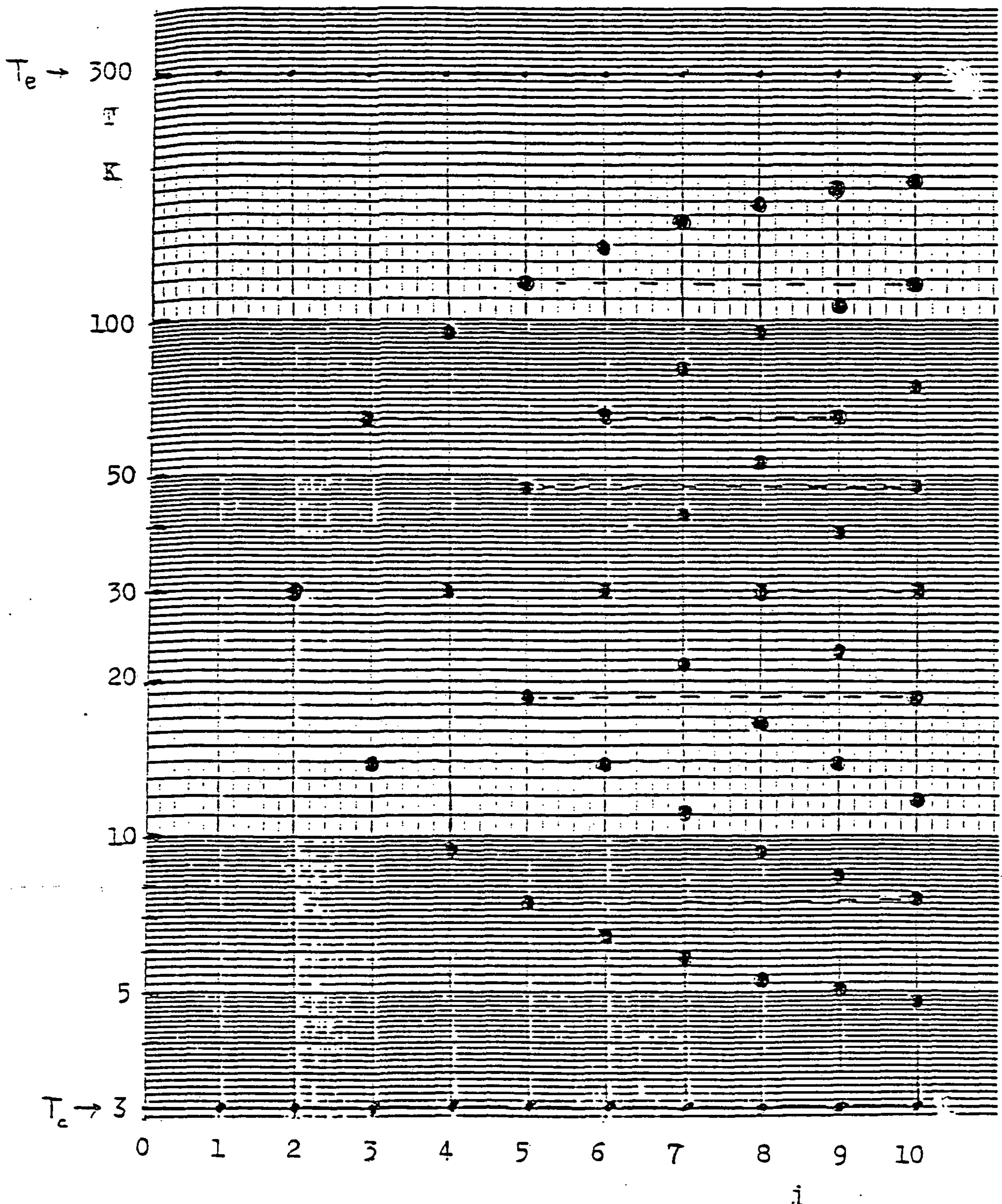

Fig. S.2. Optimum intermediate temperatures of shields vs. j ;(T_e = 300 K, T_c = 3 K).

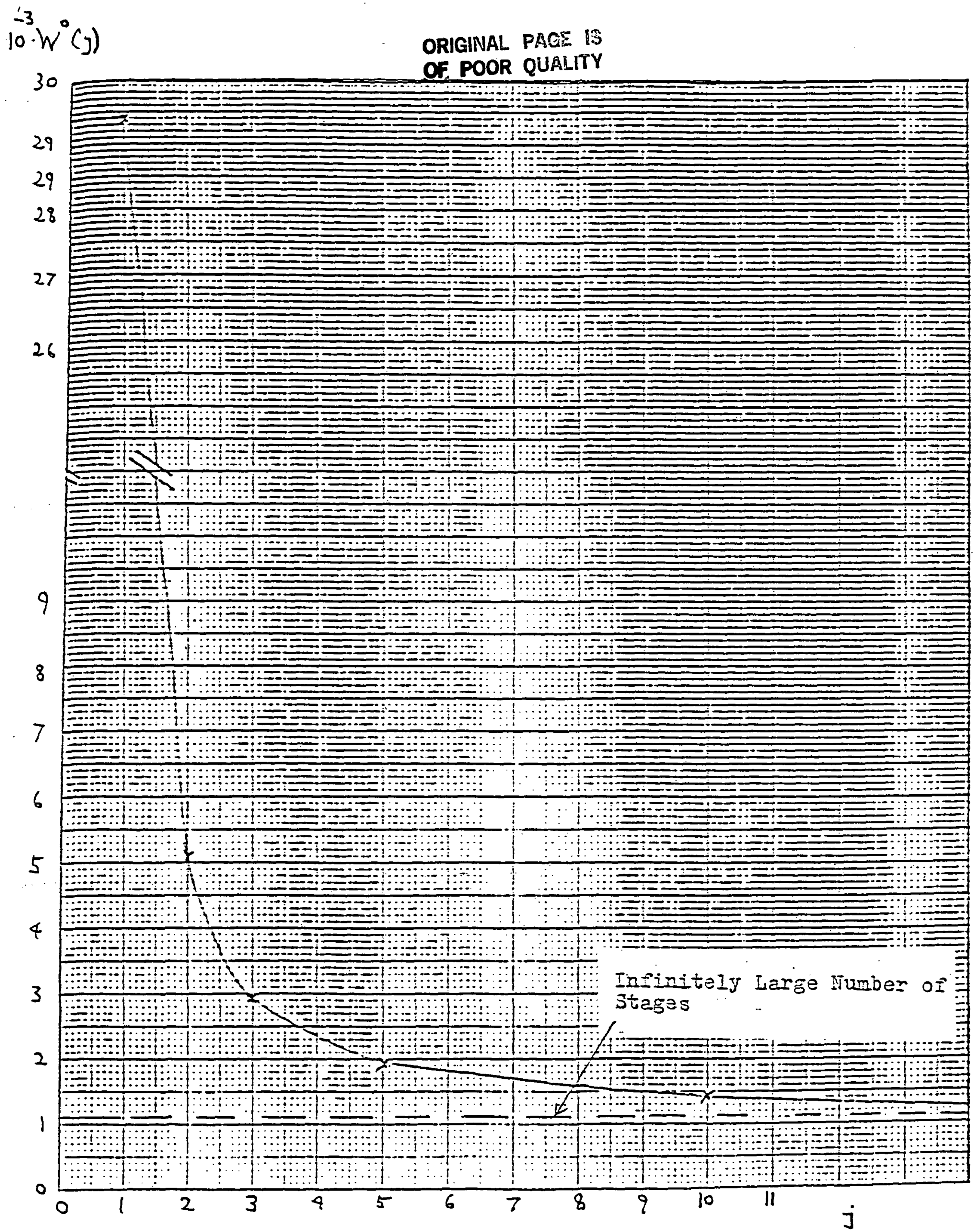

Figure S.3. Normalized power W^{o}, in dimensionless power units vs. number of stages (j); T_e= 300 K: T_c= 3 K .

SUMMARY

We have analyzed advanced dynamic insulation systems from a thermodynamic point of view. A particular performance measure is proposed in order to characterize various in - sulations in a unique manner. This measure is related to a base quantity, the refrigeration power ratio. The latter is the minimum refrigeration power, for a particular dynamic insulation limit, to the actual reliquefaction power associated with cryoliquid boiloff . This ratio serves as reference quantity which is approximately constant for a specific "ductless" insulation at a chosen NBP*. Each real container with support structure, vent tube, and other transverse components requires a larger refrigeration power. The ratio of the actual experimental power to the theoretical value of the support-less system is a suitable measure of the entire insulation performance as far as parasitic heat leakage is concerned. The present characterization is illustrated using simple thermodynamic system examples including experiments with liquid nitrogen. Numerical values are presented and a comparison with liquid helium is given.

*) Normal boiling point.